Flood characterisation of the Haor region of Bangladesh using flood index

Asadusjjaman Suman and Biswa Bhattacharya

ABSTRACT

The paper presents the flood characterisation of the Haor region in the north-east of Bangladesh. The region consists of a system of Haors, each of which is a saucer-shaped depression and interconnected by a river system. A portion of the Haor area, known as the deeply flooded area, consisting of about 15 Haors, was chosen as the study area. A 1D2D model, with one-dimensional model for the rivers and a two-dimensional model for the Haors, was developed. Flood hydrograph characteristics such as the rising curve gradient, flood magnitude ratio (with respect to the average discharge) and time to peak were assessed for different river floods. Using these characteristics an integrated flood index (FI) was developed. The FI is an aggregated indicator based on the flood hydrograph characteristics and indicates the relative overall severity of a flood. The spatial and temporal variations of the index were investigated as well. The computed FI at different locations of the region and for different flood hazard frequencies provide a broad understanding of the flooding characteristics of the region. The developed methodology can also be applied to other river basins to analyse flooding risk provided some historical flood data are available.

Key words | Bangladesh, flood characteristics, flood index, flood risk management, Haor

Asadusjjaman Suman (corresponding author)
Institute for Applied Ecology, Faculty of ESTeM,
University of Canberra,
Australia
E-mail: Asadusjjaman.Suman@canberra.edu.au

Biswa Bhattacharya
UNESCO-IHE Institute for Water Education,
Delft,
The Netherlands

INTRODUCTION

Floods constitute about 50% of all natural disasters, and as a result, life and livelihoods are regularly affected by flooding (Guha-Sapir et al. 2004; Jonkman & Kelman 2005; Jonkman et al. 2009; Vos et al. 2010). Moreover, with the population growth, urbanisation and climate change the flooding situation is being exacerbated (Reynard et al. 2001; De Moel et al. 2011; Taylor et al. 2013). Bangladesh is situated in South Asia and is one of the largest deltas of the world, formed at the confluence of the world's three major rivers – Ganges, Brahmaputra and Meghna (Mirza 2003). The occurrence of water-induced disasters is a regular phenomenon in Bangladesh (Paudyal 2002); living with floods is not an option but a way of life.

Flash, pluvial, fluvial and coastal floods are observed in Bangladesh (Ahmed & Mirza 2000). Flash floods occur during the pre-monsoon period (March–May) and are observed in the north-eastern region due to intense rainfall in the neighbouring hilly regions in India. Rain-fed flood is

caused by drainage congestion and heavy rainfall. River floods result from snow-melt in the Himalaya and heavy monsoon rainfall over the Himalaya, Assam Hills, Tripura Hills and the upper Brahmaputra and Ganges floodplains. Coastal flooding mostly occurs during the pre-monsoon and post-monsoon season.

Among the different regions of Bangladesh, the north-eastern part, known as the Haor region, has a different landscape, land use and hydrological characteristics and is not yet fully benefited from the national flood forecasting system (Chowdhury 2000). The region is bordering India and thereby has trans-boundary issues as well. The data sharing between the two countries has scope for improvement (Refsgaard et al. 1988). Moreover, the catchments on the Indian side have hilly terrain, receive a large amount of rainfall and are mostly ungauged. Numerical models of the Haor region using rainfall and water level information from the territories of Bangladesh provide limited forecast

lead time. Simulation models developed in this research show that for a number of locations of the Haor region the forecast lead time is within 6 h. Based on the geographic location of the catchment and the data scarcity, it is anticipated that hydrological and hydraulic modelling of the region will not be sufficient to manage risk from flooding. As an alternative, we seek to gather information from past flood hydrographs with a view to improving our understanding about the flooding characteristics of the region. Following the approach of Ahn & Choi (2013) and Bhaskar et al. (2000), we planned to develop a flood index (FI) based on the characteristic of flood hydrographs and subsequently, to characterize the flood severity at different locations of a catchment with the computed FI. The spatial and temporal variation of the FI with varying flood hazard magnitudes may be a useful tool in flood risk management.

STUDY AREA AND DATA

The north-eastern region of Bangladesh, which is the study area, consists of many Haors. Haors are almost round/elliptical shaped tectonically depressed marshy lands. There are about 411 Haors covering an area of about 19,700 km² with about 23 trans-boundary rivers that enter Bangladesh (CEGIS 2011). Owing to the intense rainfall at the upper catchment area with hilly topography, the rivers carry floodwater quickly to downstream (Soja & Starkel 2007), which leads to flooding in the Haor region. The upstream catchments in India receive heavy rainfall and include the world's highest rainfall occurring location Cherapunjee. The Haor region is drained mainly by the Surma–Kushiyara river system (Figure 1).

A Haor is used during the dry period (December–mid–May) for agriculture and as a fishery during the wet period (June–November). Boro rice is the main crop of the region. The pre-monsoon flooding, which occurs during April and May, can cause loss of crops of the entire year and increases the risk to the economic, social and environmental sectors of the Haor region (IWM 2007). Most Haors are protected with embankments constructed by the Bangladesh Water Development Board. The purpose of the embankments is to protect Haors' crop from pre-monsoon flooding. The embankments are of low height, which can protect the area

against minor floods, but not major floods (IWM 2007). During monsoon most of the embankments become inundated. Repeated floods over the last few years have also weakened the existing embankments, and poor maintenance causes breaching during flooding.

The Haor region, particularly its flooding characteristics, has not been studied well. Taro et al. (2002) simulated the behaviour of Hakaluki Haor for the flood of 1988. They observed that water comes into the Hakaluki Haor from the Kusiyara River in May until the water level of the Hakaluki Haor reaches almost the same level as the Kusiyara River. The water depth was 6.9 m in the middle of the Hakaluki Haor and approximately 2 m in the periphery of the Hakaluki Haor area. The Hakaluki Haor maintained a high water level until the beginning of October. Water moved out through the Kusiyara River from October and, by 15 November 1988, the water level reached almost the same level as that on 1 May.

The entire Haor region is too large for a detailed study, particularly involving two-dimensional (2D) modelling, which demands long computing time. Accordingly, a portion of the Haor region, known as the deeply flooded Haor area (Figure 1), was considered in this research. The deeply flooded Haor area consists of 15 Haors. The entire Haor region is fed mainly by three Indian catchments, namely Meghalaya, Barak and Tripura. The deeply flooded Haor area is defined by the region fed mainly by the Meghalaya catchment of India.

All observed data were collected from following eight upstream stations of the deeply flooded Haor area Kanairghat (Station ID 266), Protappur (Station ID 233) and Sheola (Station ID 173) located in Sylhet, Durgapur (Station ID 263), Uragaon (Station ID 337) and Islampur (Station ID 332) located in Netrokona, Muslimpur (Station ID 333) and Laurergarh Saktiarkhola (Station ID 131.5) located in Sunamgonj. The length of the data record is 30 years from 1980 to 2010 and the time step of observation is 3 h.

METHODOLOGY AND MODELS

The complexity of the hydrological/hydraulic interaction between the river system and the Haors means that understanding the system is quite difficult. As a result,
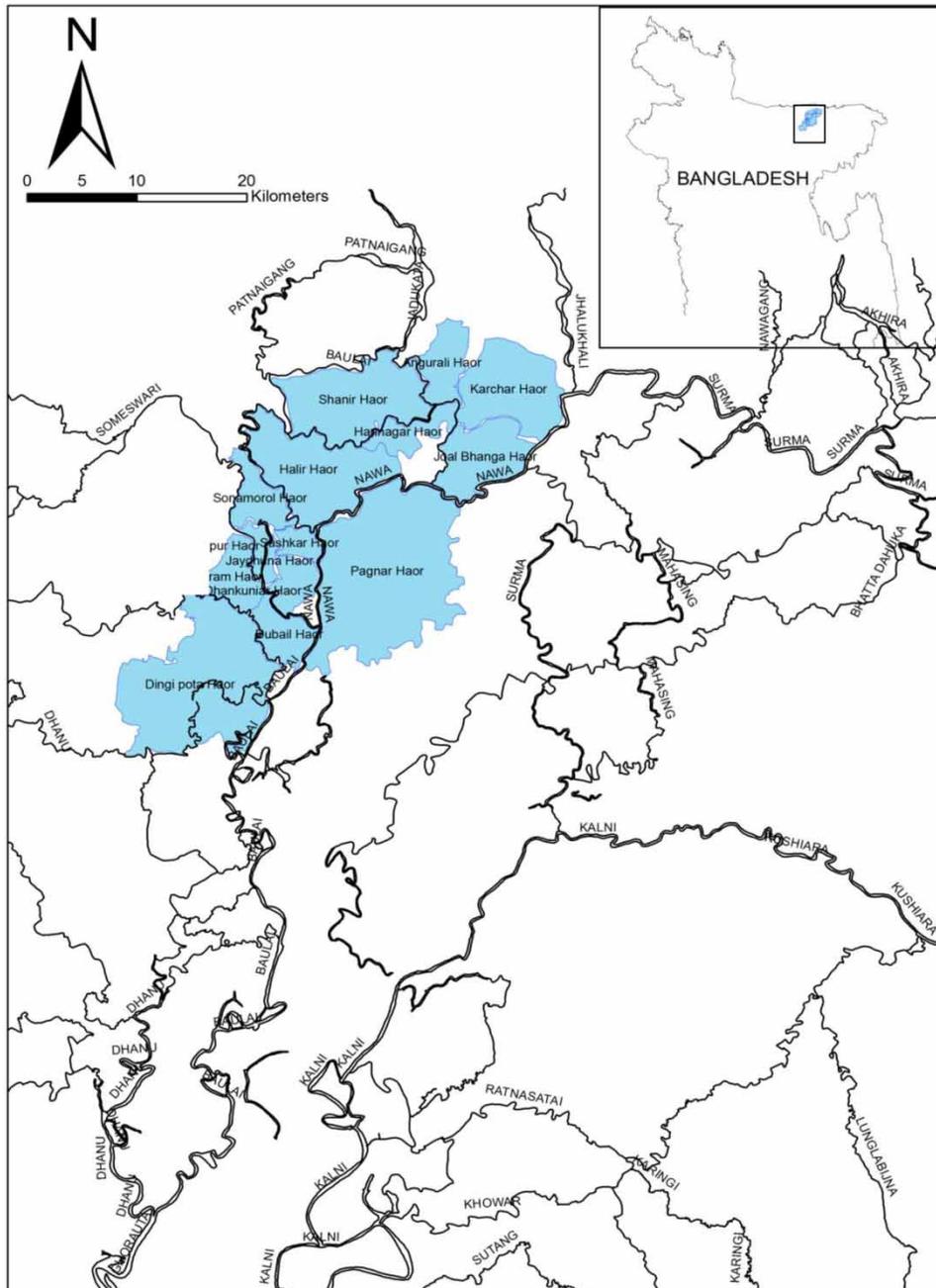
Figure 1 | The deeply flooded area of the Haor region with the major river system, which is used as the study area.

characterisation of floods and planning and designing mitigation measures are difficult. To simulate the flooding extent in the rivers and Haors, a numerical model was developed. The river system was modelled with a one-dimensional (1D) model; whereas the Haors were modelled with a 2D model. The numerical modelling tool MIKE11 (DHI 2003) was used to develop a 1D hydrodynamic model of the river system in the study area. MIKE11 is an integrated river and channel modelling tool that solves the Saint Venant equations of continuity and momentum to compute the water level and discharge in space and time along rivers. More detailed descriptions of the shallow water equations

and their numerical solutions can be found in Cunge *et al.* (1980), and the issues related to the practical implementation of the tool can be found in DHI (2003).

Available gauge discharge data were used in providing the upstream boundary condition for all the rivers connected to the deeply flooded Haor area. Water level obtained from the gauge station near Chandpur at Upper Meghna River was used as the downstream boundary condition.

The 2D model was used to measure the depth and extent of flooding in the Haors. This model was developed using MIKE21 (DHI 2012) modelling system. The digital elevation model (DEM) was created using the satellite data of 90 m × 90 m resolution from shuttle radar topography mission, augmented with some field surveys. To be able to represent the embankments around the periphery of each Haor, which have narrow widths, two types of computational mesh were developed for using in the 2D model. A rectangular mesh was used for embankments and a triangular flexible mesh was used for the rest of each Haor area.

A MIKE-Flood model was developed by integrating the 1D and 2D models. Twelve rivers were laterally linked by 36 reaches and 489 points. The 1D model was calibrated with respect to the observed discharge from a number of gauges of the study area. During the calibration the root mean squared error (RMSE) between the simulated and measured discharge was minimised using the following equation:

$$\text{RMSE} = \sqrt{\frac{1}{N}\sum_{i=1}^{N}(Q_{\text{obs},i} - Q_{\text{sim},i})^2} \quad (1)$$

where $Q_{\text{obs},i}$ is the *i*th observed discharge, $Q_{\text{sim},i}$ is the corresponding simulated discharge and $i = 1,2,3,\ldots,N$ where N is the total number of observations in the calibration period.

The calibration data of the 2004 flood showed substantial variation of water levels in the various rivers in the modelled domain. For example, the water level in the Surma River varied from 2.7 to 9.08 m. The calibrated model was used with RMSE of 0.669 m. The calibrated friction parameter (Manning) varied for the rivers between 0.022 and 0.033 m$^{-1/3}$s with a value of around 0.025 m$^{-1/3}$s for most rivers. However, for a limited number of river reaches, for example River Baulal at chainage 25,000 and River Jaduka at chainage 21,000, the calibrated Manning's
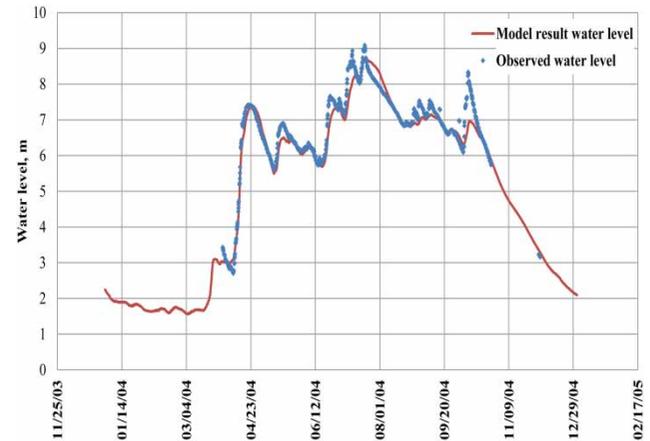

Figure 2 | Observed and modelled water level in the Surma River.

parameter was 0.1 m$^{-1/3}$s. As the calibration data were from only a year we do not know about the sensitivity of the friction parameter in the modelled domain. Figure 2 shows the model and observed water level at the upstream of the Surma River during the 2004 flood.

The 2D model was calibrated to a limited extent with remote sensing images of the Haor area. The flood extent simulated by the 2D model was compared with the flood extent from SATIS satellite image (CEGIS 2011). However, it was not possible to ascertain the depth of flood from the satellite image. So, the 2D model was compared to only the flood extent of satellite images. From the analysis of the satellite image and model results, it was concluded that the flood extent simulated by the model was close to the flood extent depicted on the satellite imagery. The limitation of flood extent data restricted the proper calibration of the 2D model, and this issue will be taken up later. However, in this paper we are using the results of the 1D model and therefore, the accuracy of the 2D model should not influence the findings.

A procedure for characterising the flood severity by defining a FI for each river based on the characteristics of the shape of flood hydrographs was developed by modifying the approach of Bhaskar *et al.* (2000) and Ahn & Choi (2013). Important information about the flooding characteristics can be determined from the flood hydrograph. In particular, the steepness of the rising limb of the hydrograph, the peak flood magnitude and the time to reach the flood peak carry important information of flooding characteristics (Bhaskar *et al.* 2000). These characteristics of the

flood hydrograph are described by the rising curve gradient, the flood magnitude ratio and the time to peak and are defined below.

Rising curve gradient (K)

The rising curve gradient conceptually is related to the steepness of the rising limb of the hydrograph and can be approximately described by an exponential equation of the following general form (Bhaskar *et al.* 2000):

$$Q_p = Q_0 e^{Kt} \tag{2}$$

where Q_0 is the initial discharge, Q_p is the peak discharge at a later time t, K is the rising curve gradient (day^{-1}), and t is time in days.

The rising curve gradient is a measure of the steepness of the rising limb of the flood hydrograph and, hence, higher K values are associated with rapidly rising floods. The value of K is a typical characteristic of a river. It depends upon the river geometry, longitudinal slope, hydrodynamics, sediment and flooding characteristics. Its value may decrease in the downstream direction although the actual decrease depends upon the flood attenuating properties of the channel. Figure 3 shows the conceptual approximation of the rising flood in Baulal River from the study area.

Similar to Bhaskar *et al.* (2000), we considered Q_0 as the time flooding starts. Defining the time flooding starts can be
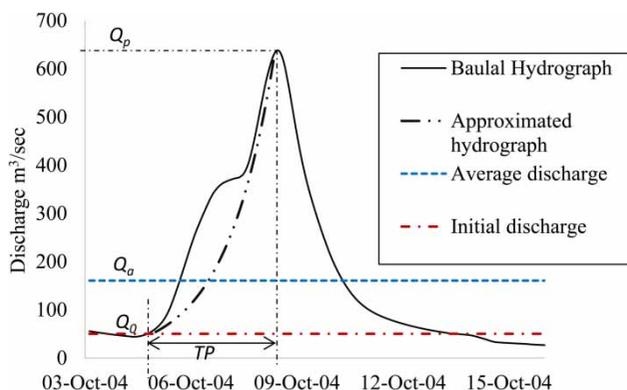

Figure 3 | A part of the flood hydrograph in Baulal River in October 2004. The approximated hydrograph is constructed using Equation (1) with $K = 0.73$. Q_p, Q_a and Q_0 denote the peak flood, average discharge and initial discharge, respectively, and TP denotes the time in days to reach the peak flood.

tricky, particularly during successive floods. However, we observed that minor mistakes in estimating Q_0 do not significantly influence FI. For the Haor region, values of K varied from 0.16 to 1.8 day^{-1} at the upstream locations. With our limited experiments we noticed that the K value for a river location in the study area did not change much between the monsoon and pre-monsoon floods.

Flood magnitude ratio (M)

The flood magnitude ratio (M) conceptually is related to the order of magnitude by which the peak flood discharge exceeds the long-term average discharge and is defined as

$$M = \frac{Q_p}{Q_a} \tag{3}$$

where Q_p is the flood peak discharge and Q_a is the long-term average discharge. In many rivers, the peak discharge may be several orders of magnitude higher than the average discharge. The parameter M expresses the severity of flooding. A larger value of M means a more severe flood. For example, the parameter M for the Nawa and Baulal rivers in the study area was about 4.2 and 11.7, respectively, at upstream locations during the monsoon flood in 2004. Similar to the parameter K, the parameter M may also decrease in the downstream direction. The extent of the decrease depends upon the flood attenuation. In this study, the flood magnitude ratio for the Haor region varied from 4.2 to 22.1 at upstream locations.

Time to peak (TP)

The parameter time to peak (TP) is defined as the duration between the time the flood event starts and the time when the peak discharge occurs. A low value of TP, associated with a high value of M, is typical of a severe flood. The parameter TP is defined as

$$TP = T_p - T_s \tag{4}$$

where T_s and T_p denote the time flood starts and the flood peak is reached. Ahn & Choi (2013) defined the start of flooding when the water level goes above the bank level.

They also considered the end of flooding as the time when the water level comes back to the bank level. This definition includes the time of slow recession of floods from the flood peak to the bank-full discharge. In flood management, we are more concerned about the peak flood. We note that the definition of Ahn & Choi (2013) leads to a higher TP. As a result, in this paper, we have considered TP as the time duration between the time flooding starts and the peak flood is reached. Note that the 2004 flood was an extreme flood with a return period of 100 years due to successive high rainfall in upper catchment. Owing to geometry of the rivers and consecutive rainfall of that area, we found in some rivers that the value of TP was quite high. In this study, values for the time to peak for the Haor region varied from 2 days to 15 days at upstream locations.

Bhaskar et al. (2000) computed FI by arbitrarily assigning numerical classes to each of the above three parameters and then by adding them. The approach is subjective and as a result it becomes difficult to compare FI values with new flooding incidents in the same catchment or with flooding in another catchment. Moreover, the sensitivity of the classification of the parameters is unknown. This aspect was improved by Ahn & Choi (2013) by normalising each parameter in a scale 0 and 1, then computing FI as the geometric mean of the three parameters. This approach partly resolves the limitation of the previous approach. However, the normalisation procedure of Ahn & Choi (2013) for the parameter TP indeed contributes to higher FI for slow rising floods.

The parameter FI is not a physical parameter that can be measured or explained with the laws of physics. It rather is an index, which can best be explained as a number relative to others. In this respect, we suggest computing FI for a standard flood, setting the value of FI for this flood as 1 and then expressing FI of other floods relative to this standard flood. As the 100-year flood is widely used in flood management studies so we recommend using the 100-year flood of a catchment as the standard flood. This means that we compute the FI value for the 100-year flood, set it as 1, and then compute FI for all other floods relative to this 100-year flood. The procedure is explained below.

The parameters K, M and TP may be computed using Equations (2)–(4), respectively. The relative severity factors RK, RM and RT are the normalised values of K, M and TP, the computation of which is explained below.

The 100-year flood hydrograph may be chosen from an existing database or by resorting to a flood frequency analysis. Let the K, M and TP values for the 100-year flood be expressed as K_{100}, M_{100} and TP_{100}, respectively. For any other flood the normalised severity factors RK, RM and RT can be computed from their K, M and TP values as

$$\left(\begin{array}{l} RK = K/K_{100} \\ RM = M/M_{100} \\ RT = TP_{100}/TP \end{array} \right) \tag{5}$$

Note that RT follows an inverse rule with TP, so that RT increases when the time to reach the flood peak decreases. Also note that as per Equation (5) the relative severity factors RK, RM and RT for a 100-year flood will be 1. Compared to floods of other frequencies, often more data and knowledge are available about a 100-year flood and therefore, relating the FI to the 100-year flood has an advantage. A 100-year flood does not necessarily always yield the same hydrograph and as a result the parameters K and TP may vary for the same 100-year flood magnitude. In that respect, the 100-year flood should be considered as the one with average catchment conditions. If due to data limitation computing FI for a 100-year flood is problematic, then the maximum flood that is available on record can be used as the standard flood in computing FI. In case a numerical model is used in generating runoff data then by varying the catchment conditions an envelope of runoff for the 100-year rainfall can be obtained from which the runoff generated with the average conditions can be considered as the standard flood for computing FI.

Note that a location needs to be associated with the FI value as it changes along rivers even for the same flood and that the parameters K_{100}, M_{100} and TP_{100} may not refer to the same location for which the FI is computed (Equation (5)) but may have been computed based on a flood hydrograph of the reference location. In flood frequency studies, it is customary to carry out frequency studies using discharge/water level data at multiple gauging locations. It may be easier to first locate the station which may serve as the reference location. Based on our knowledge of a catchment we may be able to identify the

gauging station with a high-flooding severity and select that location as the reference location. Subsequently, we can compute the parameters K_{100}, M_{100} and TP_{100} for this location and use these parameters in computing FI for any flood at any location within the catchment. Different flood hydrographs at different locations corresponding to the same flooding incident can be used to compute the parameters K, M and TP, and subsequently, their normalised versions using Equation (5). This procedure allows studying the spread of FI values in a catchment for the same flood and as a result helps in understanding the spatial variation of the flooding risk. The computation, however, does not depend on the selection of the reference location.

Once the RK, RM and RT values are computed using Equation (5), then the FI can be computed using the geometric mean of these three normalised parameters as follows:

$$FI = \sqrt[3]{(\alpha RK) \times (\beta RM) \times (\gamma RT)} \qquad (6)$$

where α, β and γ are coefficients assigned to increase or decrease weights to the three parameters. In this study α, β and γ are considered as 1. Note that if α, β and γ are considered as 1 then FI will be 1 for a 100-year flood. Larger floods may yield FI higher than 1.

The three indices are not entirely independent. For example, the parameter K and TP are interrelated and as K increases TP is expected to decrease. However, removing one also causes loss of information and therefore, the use of both parameters is practised (Bhaskar et al. 2000; Ahn & Choi 2013).

RESULTS AND DISCUSSION

The FI values were computed using Equations (2)–(6) for the rivers in the Haor region and Table 1 summarises the results with the data from the validation period. Severe flooding in the Jaduka River was observed in the past and accordingly, station *Laurergarh Saktiarkhola* (Station ID 131.5) on this river was chosen as the reference location. The annual maximum discharge data of this station for the period 1980–2010 were used to fit a Gumbel distribution and the 100-year flood was computed to be 3497 m³/s. During the 2004 flood, the peak flood discharge at the same station was 3475 m³/s, which is close to the 100-year flood and accordingly, the indexing parameters for the 2004 flood for this station has been chosen as 1. The FI values at others locations were computed using Equation (5).

Table 1 | Summary of flood indices of different rivers in the Haor region

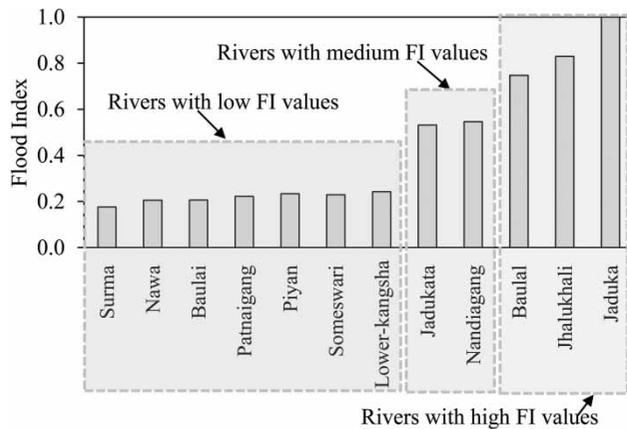| River name	Initial discharge Q_0 (m³/sec)	Peak discharge Q_t (m³/sec)	Average annual discharge (m³/sec)	Rising curve gradient (K)	Flood magnitude ratio (M)	Time to peak (TP) days	Normalised rising curve gradient (K) day⁻¹	Normalised flood magnitude ratio (M)	Normalised time to peak (TP) days	Normalised flood index (FI)
Jhalukhali	175	3025	200	1.425	15.13	2	0.80	0.68	1.00	0.83
Jaduka	100	3475	157	1.774	22.13	2	1.00	1.00	1.00	1.00
Jadukata	35	350	32	0.768	10.94	3	0.43	0.49	0.67	0.53
Baulal	50	630	54	1.267	11.67	2	0.75	0.53	1.00	0.75
Patnaigang	75	425	52	0.173	8.17	10	0.10	0.37	0.20	0.22
Nandiagang	100	1187	106	0.825	11.20	3	0.46	0.51	0.67	0.55
Surma	1000	5000	1240	0.189	4.44	9	0.11	0.20	0.22	0.18
Nawa	400	5000	1200	0.316	4.17	8	0.18	0.19	0.25	0.21
Baulai	900	5352	1000	0.223	5.35	8	0.13	0.24	0.25	0.21
Piyan	10	57	6	0.158	9.50	11	0.09	0.43	0.18	0.23
Someswari	500	5609	548	0.161	10.24	15	0.09	0.46	0.13	0.23
Lower-kangsha	30	140	20	0.220	7.00	7	0.12	0.32	0.29	0.24

Figure 4 | Categories of different rivers on the basis of computed FI.

Based on the computed FI values, rivers were categorised. The analysis of the FI values revealed broadly the presence of three types of rivers in the study area (Figure 4). They are termed here as rivers with high FI, medium FI and low FI values. Clustering the rivers into three groups, similar to many clustering problems, is somewhat arbitrary. Interested readers may think of resorting to, for example, fuzzy C-means clustering to see the sensitivity of the grouping (Pyle 1999). However, in this paper we wanted to explore a simple approach. Moreover, the variation of the FI values for the rivers and the number of rivers itself do not perhaps justify a more complex process. Note that, higher FI values are connected to higher risks of flooding, either due to a higher flood peak, or a higher rate of increase of flood discharge with time, or a shorter time to reach the peak. Unless we refer to the individual parameters used in computing the FI, it is not possible just from the FI value to deduce which of the three parameters caused a higher (or lower) risk. Brief characteristics of the three groups are described below.

Rivers with low FI values

The following rivers Surma, Nawa, Baulai, Patnigang, Piyan, Someswari and Lower-Kangsha in the study region have FI values less than 0.25 and belong to this group.

The flood hydrographs, in general, show a slow rise in these rivers (i.e. low K and/or high TP values). For this group, value of K and TP varies between 0.16 and 0.32, and

7 and 15 days, respectively. For example, the Nawa River belongs to this group and is a slow response river of the region. The average values of M and TP were about 4.2 and 8 days, respectively. Figure 5(a) shows the propagation of the 2004 flood in the Nawa River and depicts that the pre-monsoon flood started on 14 April 2004. It also shows that the flood wave was attenuated considerably at the downstream reach of the river.

On an average, for this group of rivers, the attenuation of the peak flood discharge was about 40% at the downstream reach of the river compared to the upstream flood discharge. The average distance between the upstream and the downstream was about 175 km. Wit et al. (2007) have shown the attenuation of the flood in Meuse River from Borgharen in Belgium to Megen in the Netherlands during the flood of 1994, 2002 and 2003 and the corresponding reduction of flood risk due to the attenuation. The attenuation of flood peak reduces the flood risk at the downstream reaches of the river. For example, in the Nawa River the FI was 0.21 at the upstream; whereas, the FI at the downstream was 0.15. A similar phenomenon has been observed in all other rivers of this group.

Rivers with medium FI values

The rivers Jadukata and Nandigang in the region have FI values 0.53 and 0.55, respectively, and have been considered to belong to the group of rivers with medium FI values.

For this group of rivers the flood hydrograph rises faster than the previous group (i.e. high K and/or low TP values). For this group, values of K and TP are about 0.8 and 3 days, respectively. For example, the Nandiagang River belongs to this group and is a quick response river of the region. The average values of M and TP were 11.2 and 3 days, respectively. Figure 5(b) shows the propagation of the 2004 flood in Nandiagang River. The attenuation of flood discharge at the downstream reaches was much less compared to the slow response rivers. This can partly be explained by the fact that the river slope of Nandiagang (or other rivers of this group) is higher compared to that of the slow response rivers. The attenuation of the peak discharge of rivers of this group was observed to be only about 5% (in a length of about 200 km). Figure 5(b) depicts multiple peaks in the
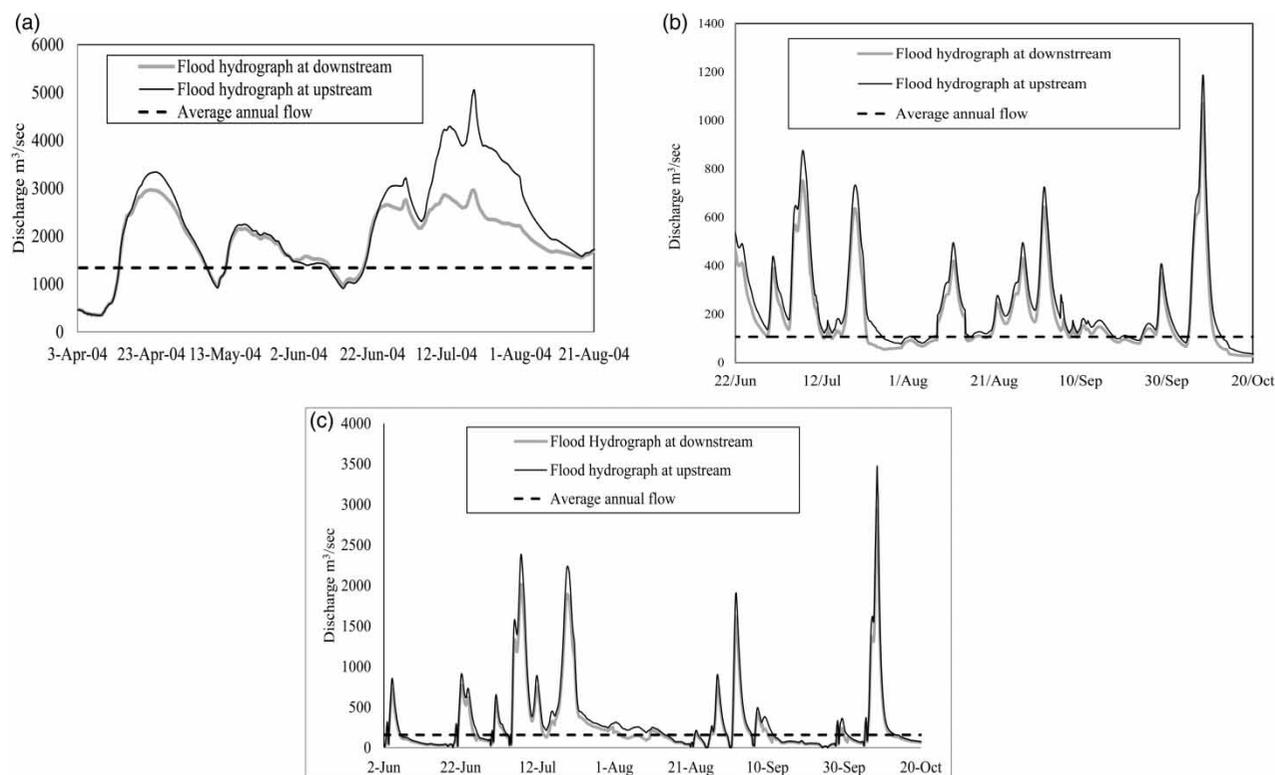
Figure 5 | Comparison of hydrographs of the (a) Nawa, (b) Nandiagang and (c) Jaduka rivers at upstream and downstream locations during the 2004 flood.

flood hydrograph; similar characteristics of the hydrograph have been observed also in other rivers of this group.

Rivers with high FI values

The rivers Baulal, Jaduka and Jhalukhali in the region have FI values equal or greater than 0.75 and have been considered to belong to the group of rivers with high FI values.

For this group of rivers, the flood hydrograph rises very fast. For the 2004 flood the K, M and TP parameters also reveal the reason for high FI values for these rivers (Table 1). The value of K and M varies between 1.3 and 1.8, and 11.7 and 22.1 were the highest in the region. The values of TP were 2 days for all rivers in this group. Figure 5(c) depicts the propagation of the 2004 flood in the Jaduka River. Analysis of the propagation of the 2004 flood in this river shows that the attenuation of the peak flood discharge at the downstream end compared to the upstream flood discharge was only about 4%, which can be partly justified by the high river bed slope of these rivers.

Spatial and temporal variation of FI

Using the results of the numerical models, the FI values were computed at a number of locations along each of the various rivers of the study region (Figure 6). It is discernible from Figure 6 that the FI values decrease along the rivers. The extent of the decrease depends very much upon a river's characteristics (e.g. geometry). For example, in Jaduka River, the FI value decreased from 1.00 to 0.81 in about 200 km, whereas in Nawa River for the same distance the FI value decreased from 0.21 to 0.15. So, it is possible that a river, falling under one of the three groups mentioned above (Figure 4), may, at a different location, appear in another group. Note that the particular characteristics of the variation of FI as shown in Figure 6 are very specific to the catchment under consideration. In the Haor catchment, more than 60% of water comes from the upstream Indian catchments and less than 40% of water is due to rainfall in the Haor catchment (Mirza 2003). Also, due to the hilly terrain of the Indian catchments and due to the
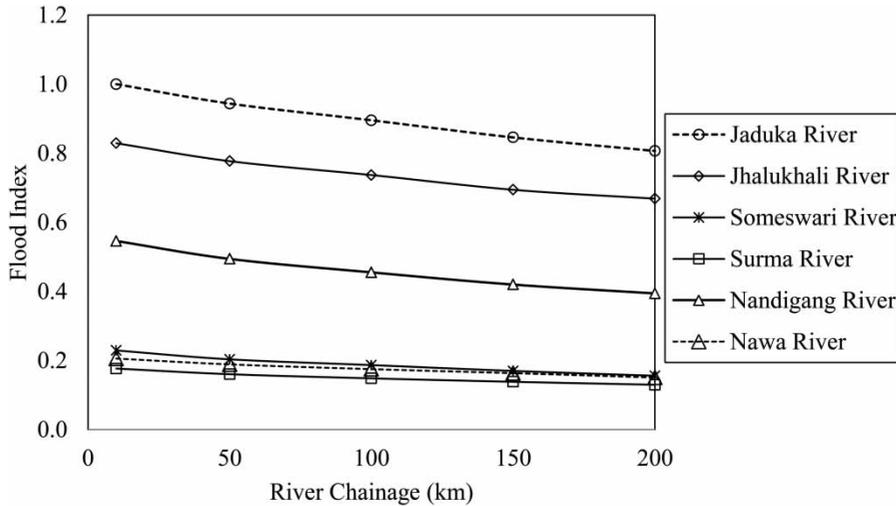
Figure 6 │ Spatial distribution of flood indices in different rivers of the Haor region.

presence of many torrents in the Indian side, floods in the upstream part of the Haor catchment rise relatively fast. As it moves downstream, the Haors provide large flood-plains to partially accommodate the flood water. For another catchment it is not unlikely to see that the FI values increase in the downstream direction of rivers.

As FI is developed from hydrograph characteristics so in principle it would vary with floods of different return periods. By carrying out regional flood frequency analysis (Haddad *et al.* 2012; Del Giudice *et al.* 2013; Rahman *et al.* 2013) of the Haor region, floods of different return periods were computed. The parameters K, M, and TP were computed for the peak flood discharge of different return periods. Using Equations (2)–(6), the FI values of all the rivers were computed for floods of different return periods (Figure 7). Note that, for example, Jhalukhali River, which was categorized as a river with a high FI value for the 2004 flood, belongs to the group of medium FI values for a flood of 10 years return period. The spatial variation (Figure 6) and temporal variation (Figure 7) of FI values of
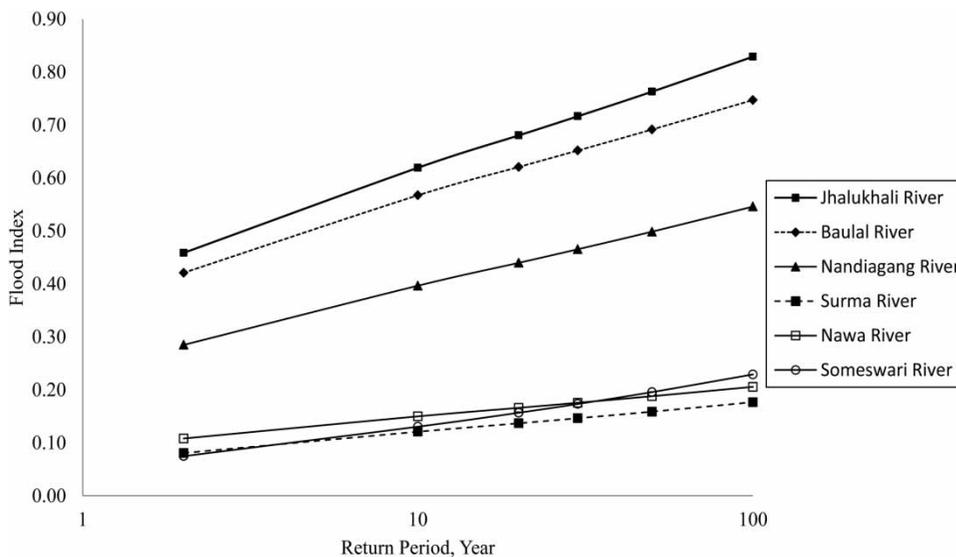

Figure 7 │ Temporal distribution of flood indices in different rivers of the Haor region.

the catchment provides a brief summary of the flooding characteristics of the Haor region.

CONCLUSIONS

The paper presents the development of a FI using the results from numerical models and the characterisation of flooding of the Haor region of Bangladesh using the developed index.

A procedure for computing FI to express the severity of flooding is presented. The FI was computed using the characteristics of flood hydrographs. In particular, the steepness of the rising limb of the hydrograph, the flood magnitude ratio, and the time to peak were considered. The computed FI was normalised with respect to a standard flood and the 100-year flood has been considered as the standard flood. As a result the computed FI provides its relative severity compared to the 100-year flood of the catchment.

Based on the clustering of the FI values, three groups of rivers were noticed in the studied region rivers with low FI, medium FI and high FI. The spatial variation of FI was computed, which showed the gradual decrease of FI along different rivers. A flood frequency study was carried out and FI for floods of different return periods were computed to investigate the progression of FI values with different flood hazard probability. The spatial and temporal variation of the FI values in the catchment provides an indicative assessment of risk from flooding, computed in relation to the 100-year flood.

This technique can be used for effective flood management, flood insurance studies and planning for emergency evacuation during flood.

ACKNOWLEDGEMENTS

REFERENCES

Ahmed, A. U. & Mirza, M. M. Q. 2000 Review of causes and dimensions of floods with particular reference to flood '98: national perspectives. In: *Perspectives on Flood 1998* (Q. K. Ahmad, A. K. A. Chowdhury, S. H. Imam & M. Sarkar, eds). Dhaka University Press Ltd, Dhaka, Bangladesh, pp. 67–84.

Ahn, J. H. & Choi, H. I. 2013 A new flood index for use in evaluation of local flood severity: a case study of small ungauged catchments in Korea. *J. Am. Water Resour. Assoc.* **49** (1), 1–14.

Bhaskar, N. R., French, M. N. & Kyiamah, G. K. 2000 Characterization of flash floods in Eastern Kentucky. *J. Hydrol. Eng.* **5** (3), 327–331.

CEGIS (Center for Environmental and Geographic Information Services) 2011 *Master Plan of Haor Area*. Bangladesh Haor and Wetland Development Board, Ministry of Water Resources, Government of Bangladesh, Dhaka.

Chowdhury, R. 2000 An assessment of flood forecasting in Bangladesh: the experience of the 1998 flood. *J. Nat. Haz.* **22**, 139–163.

Cunge, J. A., Holly, F. M. & Verwey, A. 1980 *Practical Aspects of Computational River Hydraulics*. Pitman Advanced Publication, Boston.

Del Giudice, G., Padulano, R. & Rasulo, G. 2013 Spatial prediction of the runoff coefficient in Southern Peninsular Italy for the index flood estimation. *J. Hydrol. Res.* **45** (2), 263–281.

De Moel, H., Aerts, J. C. J. H. & Koomen, E. 2011 Development of flood exposure in the Netherlands during the 20th and 21st century. *J. Global Envir. Change* **21** (2), 620–627.

DHI (Danish Hydraulic Institute) 2003 Short introduction tutorial: MIKE 11 – a modelling system for rivers and channels. Available from: www.tu-braunschweig.de/Medien-DB/geooekologie/mike-11-short-introduction-tutorial.pdf (last accessed 14 February 2014).

DHI (Danish Hydraulic Institute) 2012 *MIKE 21 Quick Start Guide – Flexible Mesh Series*. DHI Water and Environments (UK) Ltd, Reading, UK.

Guha-Sapir, D., Hargitt, D. & Hoyosis, P. 2004 *Thirty Years of Natural Disasters 1974–2003: The Numbers*. Centre for Research on the Epidemiology of Disasters, Belgium.

Haddad, K., Rahman, A. S. & Stedinger, J. 2012 Regional flood frequency analysis using Bayesian generalized least squares: a comparison between quantile and parameter regression techniques. *J. Hydrol. Process.* **26** (7), 1008–1021.

IWM (Institute of Water Modelling) 2007 *Mathematical Modelling along with Hydrological Studies and Terrestrial Survey under the Haor Rehabilitation Scheme – Final Report*. March 2007. Institute of Water Modelling, Dhaka, Bangladesh.

Jonkman, S. N. & Kelman, I. 2005 An analysis of causes and circumstances of flood disaster deaths. *J. Disasters* **29** (1), 75–97.

Jonkman, S. N., Maaskant, B., Boyd, E. & Levitan, M. L. 2009 Loss of life caused by the flooding of New Orleans after Hurricane Katrina: analysis of the relationship between flood characteristics and mortality. *J. Risk Analysis* **29** (5), 676–698.

Mirza, M. M. Q. 2003 Three recent extreme floods in Bangladesh: a hydro-meteorological analysis. *J. Nat. Haz.* **28**, 35–64.

Paudyal, G. N. 2002 Forecasting and warning of water-related disasters in a complex hydraulic setting – the case of Bangladesh. *J. Hydrol. Sci.* **47** (S1), S5–S18.

Pyle, D. 1999 *Data Preparation for Data Mining*. Morgan Kaufmann, California.

Rahman, A. S., Haddad, K. & Rahman, A. 2013 Regional Flood Modelling in the New Australian Rainfall and Runoff. In: *MASSANZ/IMACS Biennial Conference on Modelling and Simulationh, 1–6 December, 2013*, Adelaide, Australia.

Refsgaard, J. C., Havno, K., Ammentorp, H. C. & Verwey, A. 1988 Application of hydrological models for flood forecasting and flood control in India and Bangladesh. *J. Adv. Water Resour.* **11** (2), 101–105.

Reynard, N. S., Prudhomme, C. & Crooks, S. M. 2001 The flood characteristics of large U.K. Rivers: potential effects of changing climate and land use. *J. Clim. Chang.* **48**, 343–359.

Soja, R. & Starkel, L. 2007 Extreme rainfalls in Eastern Himalaya and southern slope of Meghalaya Plateau and their geomorphologic impacts. *J. Geomorphol.* **84** (3–4), 170–180.

Taro, O., Iguchi, M., Ahmed, S. M. U. & Bala, S. K. 2002 Numerical simulation of flood lake behaviour in northeastern Bangladesh. In: *Proceedings of the 13THAPD IAHR Congress, August, 2002*, Singapore, Vol. 1, 528.

Taylor, J., Biddulph, P., Davies, M. & Lai, K. M. 2013 Predicting the microbial exposure risks in urban floods using GIS, building simulation, and microbial models. *J. Envir. Int.* **51**, 182–195.

Vos, F., Rodriguez, J., Below, R. & Guha-Sapir, D. 2010 *Annual Disaster Statistical Review 2009 – The Numbers and Trends*. Centre for research on the Epidemiology of Disasters, Belgium.

Wit, M. J. M. D., Peeters, H. A., Gastaud, P. H., Dewil, P., Maeghe, K. & Baumgart, J. 2007 Floods in the Meuse basin: Event descriptions and an international view on ongoing measures. *Int. J. River Basin Manage.* **5** (4), 279–292.